Translin Binding to DNA: Recruitment through DNA Ends and Consequent Conformational Transitions

Kundan Sengupta and Basuthkar J. Rao*

Department of Biological Sciences, Tata Institute of Fundamental Research, Homi Bhabha Road, Bombay 400 005, India

Received July 1, 2002; Revised Manuscript Received October 23, 2002

ABSTRACT: The human translin protein binds a variety of sequences (chromosomal breakpoint consensus sequences, their sequence variants, as well as nonbreakpoint sequences such as simple AT and GC repeats) at nanomolar protein concentration when short single strands (∼20−30mers) are used as DNA targets. The protein, which is known to exist as an octamer in its free state, undergoes a conformational transition upon binding to short single strands leading either to a compaction or to the dissociation of the oligomer. Moreover, the protein oligomers tend to aggregate into complexes that get progressively larger as the length of the single-stranded DNA target increases. The protein loads onto duplexes via the free ends of DNA, generating higher oligomeric complexes as a function of protein concentration. Interestingly, the conformation of DNA targets encased by translin oligomer is significantly altered such that the single strand is rendered hypersensitive to DNase I. Furthermore, the loading of translin oligomers leads to tighter clamping of duplex ends. All of these observations, taken together, suggest that translin is a bona fide binder of DNA ends, thereby subjecting the DNA to a conformation conducive for repair steps during translocation events. We discuss the results in the perspective of translin biology.

Chromosomal translocations are involved in the genesis of a variety of lymphomas and leukemias. Studies have shown that novel conserved sequence motifs such as ATG-CAG and GCCC(A/T)(G/C)(G/C)(A/T), with gaps and intervening nucleotides, are present at the 5′ flanking sites of the breakpoint junctions of various chromosomal translocations in human lymphoid neoplasms (*1*, *2*). Extensive molecular analyses led to the identification of a novel protein called translin from [TCR $\beta\delta$] T cell leukemia nuclear extracts which specifically binds to conserved sequences at chromosomal breakpoint junctions (*1*).

Translin is a highly conserved 27 kDa protein that binds specific RNA and DNA targets (*1*, *3*). The mouse orthologue of translin, testis brain RNA binding protein (TB-RBP), was identified as an RNA binding protein in testis and binds to conserved sequence elements in the 3′ untranslated regions of mRNAs. Therefore, a role of translin in translational regulation and RNA movement has been suggested. Translin has been shown to interact with proteins such as GADD, translational ER ATPase, cytoskeletal G-actin, and trax (*4*, *5*). Trax is a 32 kDa protein that enhances translin binding to DNA (*6*). TB-RBP also contains a highly conserved putative GTP binding site at its C-terminal end (*7*). GTP, but not GDP, reduces translin binding to RNA by 50% without affecting its DNA binding ability. An alteration in the GTP binding site has a dominant negative function in transfected cells causing cell death (*7*).

Chromosomal translocations basically arise as a result of the fusion of two or more broken ends of chromosomes. The ligation of these ends, need to be actively catalyzed by proteins. The *n*on*h*omologous *e*nd *j*oining pathway (NHEJ) is one of the most crucial pathways necessary for ligating DNA ends during double strand break repair (*8*). This has been demonstrated by the extreme sensitivity of NHEJ-deficient cells toward ionizing radiation (*9*). The precise analyses of genomic breakpoints in various liposarcomas such as CML (*10*), AML (*11*), and rhabdomyosarcoma (*12*) uncovered extensive homology with translin binding consensus sequences, strongly suggesting the involvement of translin in mediating chromosomal translocations. Electron microscopic studies of translin with DNA fragments from chromosomal breakpoints have shown that translin rings specifically bind to such DNA ends (*13*). The native cytoplasmic form of translin is present in the cell lines of various lineages, while a nuclear localization was observed in lymphoid cell lines with rearranged Ig and TCR loci (*1*). The active nuclear transport of translin was shown to be initiated when a nonhematopoietic cell line (HeLa) was treated with DNA damaging agents such as mitomycin and etoposide, which further suggested that DNA damage induces a signaling pathway resulting in active nuclear transport of translin (*1*, *13*).

The translin cDNA encodes a protein of 228 amino acids and migrates as a single band at 27 kDa under reducing conditions and forms a dimer of 54 kDa under nonreducing conditions during SDS[1]−PAGE analyses (*1*, *14*, *15*). The protein has been shown to exist as a stable octamer, sustained by leucine zipper interactions between four dimers (*1*, *15*).

* To whom correspondence should be addressed. Fax: 291-22-2152110. Phone: 291-22-2152971 ext 2606. E-mail: bjrao@tifr.res.in.

[1] Abbreviations: ATP, adenosine triphosphate; BSA, bovine serum albumin; DTT, dithiothreitol; EDTA, ethylenediaminetetraacetic acid; ds-DNA, double-stranded DNA; ss-DNA, single-stranded DNA; IPTG, isopropyl β-D-thiogalactoside; SDS, sodium dodecyl sulfate.

10.1021/bi026378m CCC: $22.00
Published on Web 11/27/2002

The molecular steps that involve translin during chromosome translocations are completely unclear. Several fundamental questions regarding where and how translin fits into the double strand break repair pathway are still to be answered.

As a step in this direction, we have tried to address (1) the nature and the relevance of consensus in the DNA target sequences in relation to translin binding function and (2) the conformational changes induced within the translin−DNA complex that might relate to its chromosome breakage−rejoining pathway. We find that translin protein binds to a variety of sequences (chromosomal breakpoint consensus sequences, their sequence variants, as well as nonbreakpoint sequences such as simple AT and GC repeats) at nanomolar protein concentration when short single strands (∼20−30mers) are used as DNA targets. Interestingly, the translin oligomeric (octameric) state undergoes changes following DNA binding: shorter single strands inducing a decrease in its hydrodynamic radius whereas the long strands promoting further oligomerization. At high enough concentrations, the protein binds duplex DNA by selectively loading from the free ends, which seems to result in clamping of strands at the duplex ends. These results are rationalized through a mechanistic model that starts describing how translin function might impinge on chromosome repair biology in the cell.

MATERIALS AND METHODS

Materials. T4 polynucleotide kinase and DNase I were purchased from Amersham Life Sciences (Cleaveland, OH), and *Nsi*I was from Roche Diagnostics (Mannheim, Germany). Oligonucleotides were synthesized at DNA Technology (Aarhus, Denmark).

DNA Substrates. All of the DNA substrates used in this study were purified by electrophoresis on a 10% denaturing polyacrylamide gel (*16*). The full-length oligonucleotide was excised from the gel and eluted into 10 mM Tris-HCl (pH 8.0) and 1 mM EDTA by diffusion, followed by desalting through a SepPak C18 cartridge (*17*). The final purity was determined by 5′ end labeling using [γ-^{32}P]ATP and analyzing on a 10% denaturing polyacrylamide gel, which revealed that the oligonucleotides were more than 95% pure.

DNA Labeling and Annealing. The conditions followed are as described earlier (*18*). The oligonucleotides (100 μM, nucleotides) were 5′-end-labeled by incubating with T4 polynucleotide kinase (3 units per reaction) and [γ-^{32}P]ATP (10 μCi) in a 5 μL reaction buffer at 37 °C for 30 min. The samples were heated at 90 °C for 4 min to inactivate the enzyme. Annealed duplexes were prepared by mixing the labeled strand with its unlabeled complementary strand at a 1:1.5 molar ratio in a buffer containing 20 mM Tris-HCl (pH 7.6) and 5 mM $MgCl_2$ and heating the sample at 90 °C for 5 min, followed by slow cooling to room temperature that took about 90 min. The completion of annealing was determined by analyzing the mobility of the annealed mix on a native polyacrylamide gel, which showed that essentially the entire labeled strand was converted to duplexes with no residual single-stranded DNA. We followed the same conditions of annealing to generate unlabeled annealed duplexes where both strands were in a 1:1 molar ratio. The annealing was assessed by kinasing a small aliquot of the same followed by analysis on a native polyacrylamide gel, which revealed that, under the conditions followed, more than 90% of the strands were in annealed form.

Protein Purification. The human translin cDNA was obtained as a His-tagged clone from Dr. M. Kasai, NIH, Japan. The bacterial cells (M15pREP4) containing the translin cDNA were grown in 600 mL of Luria−Bertini media in ampicillin (100 μg/mL) and kanamycin (25 μg/mL) to an A_{600} of 0.7 at 37 °C, were induced with 2.0 mM IPTG for about 4 h, and were harvested by centrifugation. The cell pellet was resuspended in sonication buffer [50 mM sodium phosphate (pH 7.0) and 300 mM NaCl]. The cell suspension was sonicated on ice, and the lysate was centrifuged at 15 000 rpm for 20 min at 4 °C. The supernatant (20 mL) was equilibriated with 5.0 mL of a 50% slurry of Ni-NTA−agarose (previously equilibriated with sonication buffer) for 1 h at 4 °C. The slurry was loaded in a column and washed with sonication buffer until the A_{280} of the flow-through was less than 0.01. The column was washed with 20 mM imidazole prepared in sonication buffer. The protein was eluted through a linear gradient of imidazole (20−200 mM) during which 1.5 mL fractions were collected. The fractions were analyzed on an SDS−PAGE gel. The fractions containing the pure protein were pooled and dialyzed against dialysis buffer (1× phosphate-buffered saline, 10% glycerol). The protein concentration was estimated by Bradford's method using BSA as a standard.

Electrophoretic Mobility Shift Assays (EMSA). The labeled oligonucleotide (80 nM, nucleotides) was incubated with translin (at indicated concentrations; see Figure 1) in binding buffer containing 10 mM Tris-HCl (pH 7.5), 50 mM NaCl, 1 mM EDTA, 1 mM DTT, and 5% glycerol at room temperature for 20 min. Bromophenol blue (0.1%), xylene cyanol (0.1%), and sucrose (4%) was added to each sample, following which they were electrophoresed on an 8% native polyacrylamide gel in TBE buffer (89 mM Tris-HCl, 89 mM boric acid, 2 mM EDTA, pH 8.0) at 150 V for 3 h at 4 °C. All native gels were subsequently dried under vacuum, and the radioactivity was quantified using ImageQuant software on a Molecular Dynamics PhosphorImager.

Dissociation Constant. The dissociation constant of translin for various oligonucleotide substrates was determined by estimating the counts contributed by the gel-shifted complex, expressed as a percentage of the total radioactivity [% gel-shifted complex = [(counts in gel-shifted complex)/(counts in gel-shifted complex + counts in free DNA)] × 100]. The percent gel-shifted complex was plotted on the *Y*-axis against protein concentration on the *X*-axis. The values were fitted using the program Sigmaplot 5.0 to the Michaelis−Menten equation [$Y = ax/(b + x)$, where b represents the K_d or the dissociation constant], and a hyperbolic saturation curve was obtained.

Native Gel Assays To Visualize the Oligomeric State of Translin. Breakpoint and nonbreakpoint oligonucleotides (expressed in molecular concentrations as indicated in Figure 2) were incubated with translin (5.8 μM) in binding buffer (described above) (typically in 12 μL reaction volume each) at room temperature for 20 min. Sucrose (4%) was added, and the samples were resolved by electrophoresis on native polyacrylamide (5%) gel at 50 V for 6−8 h at 4 °C. The native gel was subsequently visualized by silver staining according to a standard protocol. It is pertinent to mention that, under these assay conditions, the protocol revealed only protein staining as the level of DNA used was far below the detection limit (see Figure 2B).

Table 1: Sequences of the Single-Strand DNA Targets Used in This Study[a]

SUBSTRATE	SEQUENCE
ABL1 (24-mer)	5' TTTCAGGCCGGGC**GCGGTGGCT**GA 3'
BCL1 (24-mer)	5' **GCGCTGCA**TTGGCGTGAACGAGGG 3'
BCL6 (24-mer)	5' **CTGCAC**CTGCGATGCCTTTCAGTG 3'
Bcl-CL1 (24-mer)	5' **GCCCTCCTGCCCTCCT**TCCGCGGG 3'
sY202R (24-mer)	5' TGACAAAGTGAG**ACCCTACT**ACTA 3'
UTYF (24-mer)	5' GCATCATAATATGG**ATCTAG**TAGG 3'
Dxp'1-23B (24-mer)	5' CCGCCACAGCCCTCCCCATGGGGC 3'
AT-repeat (24-mer)	5'ATATATATATATATATATATATAT 3'
GC-repeat (24-mer)	5' GCGCGCGCGCGCGCGCGCGCGC 3'
Poly-dC_{30}	5' CCCCCCCCCCCCCCCCCCCCCCCCCCCCCC 3'
Poly-dG_{30}	5' GGGGGGGGGGGGGGGGGGGGGGGGGGGGGG 3'
NBS1 (33-mer)	5' TAAATTGTGTCGAAATCCGC**GACCTGCT**CCATG 3'
NBS2 (61-mer)	5' TCGCCTGA<u>TAAATTGTGTCGAAATCCGC**GACCTGCT**</u> <u>CCATG</u>TTACTTAGCCGGAACGAGGC 3'
NBS3 (70-mer)	5' **ACGCAC**ATACTAGGCTGTATCAGCAGCAGCAGCAG CAGCAGCAGCAGCAGTTCAGTACAGTCATGACAGT 3'
NBS4 (83-mer)	5'AACGGAGATTTGTATCAT<u>CGCCTGATAAATTGTGTCGAAATCCGC</u> <u>**GACCTGCT**</u><u>CCATGTTACTTAGCCGGAACGAGGC</u>GCAGA 3'
NBS5 (121-mer)	5'GGCTTAGAGCTTAATTGCTGAATCTGGTGCT<u>CGCCTGATAAATTGT</u> <u>GTCGAAATCCGC**GACCTGCT**</u><u>CCATGTTACTTAGCCGGAACGAGGC</u>G GATTCGCGATTCCTTGATGCCTATGGTGA 3'

[a] Sequence stretches in bold correspond to chromosome breakpoint consensus motifs described in the literature (*1*, *2*). The underlined stretch in NBS2 corresponds to the sequence of NBS1. Similarly, the underlined sequences in NBS4 and NBS5 correspond to the sequence of NBS2.

Dynamic Light Scattering of Translin in the Presence of DNA. Dynamic light scattering was carried out using a Dynapro-LS molecular sizing instrument with a microsampler (Protein Solutions). The binding buffer was filtered extensively through a filtering assembly containing 20 nm filter-anodisk membranes. Oligonucleotides of the indicated concentration (legend in Figure 2C) were incubated with translin (1.5 μM) in a 25 μL reaction volume for 10−15 min at room temperature in a quartz cuvette followed by DLS analysis. The data were analyzed using Dynamics software, which reported the hydrodynamic radii (R_H) for monomodal distributions as defined by a baseline from 0.9 to 1.001.

DNA End Binding Assays. A 2.9 kb cloning vector, -pGEM7Z (35.0 μg), was partially digested with *Nsi*I (5 units) in 25 μL reaction volume for 1.0 h at 37 °C using the supplier's digestion buffer that resulted in converting a large fraction of supercoiled plasmid into nicked circular plasmid and a small fraction of sticky-ended linear DNA. The partially cut plasmid DNA (3.5 μg/20 μL) was incubated with translin (at concentrations indicated in the legend, Figure 3) in the binding buffer (described earlier) at room temperature for 20 min, followed by electrophoresis on an agarose gel (0.8%) at 50 V for 6.0 h at 18 °C and staining with ethidium bromide for 10 min.

DNA End Clamping Assay. The 5′-end-labeled NBS2 oligonucleotide was annealed either with its unlabeled complementary strand that generates a blunt-ended 61 bp duplex or with an unlabeled strand that is complementary to NBS5 that generates a tailed duplex DNA (with 5′ and 3′ overhangs) (the conditions of annealing were as described above). The duplex substrates (1.0 nM, oligonucleotide molecules) were incubated with translin (at the indicated concentrations, Figure 4) at room temperature for 20 min. The samples were subsequently challenged with a 6-fold molar excess (6.0 nM molecules) of cold competitor DNA (unlabeled NBS2) and equilibriated at room temperature for 10 min. The reaction was quenched with SDS (0.5%) and EDTA (20 mM) following which sucrose (4%) was added. The samples were electrophoresed on a 10% native polyacrylamide gel at 50 V for 5 h at 4 °C.

DNase I Hypersensitivity Assay. The 5′-labeled NBS4 (0.5 μM nucleotide) was incubated with translin (at given concentrations, Figure 6) (as described previously) following which one set was treated with DNase I (1.25 ng/μL or 3.1×10^{-3} units/μL) and the other with an equal volume of 10

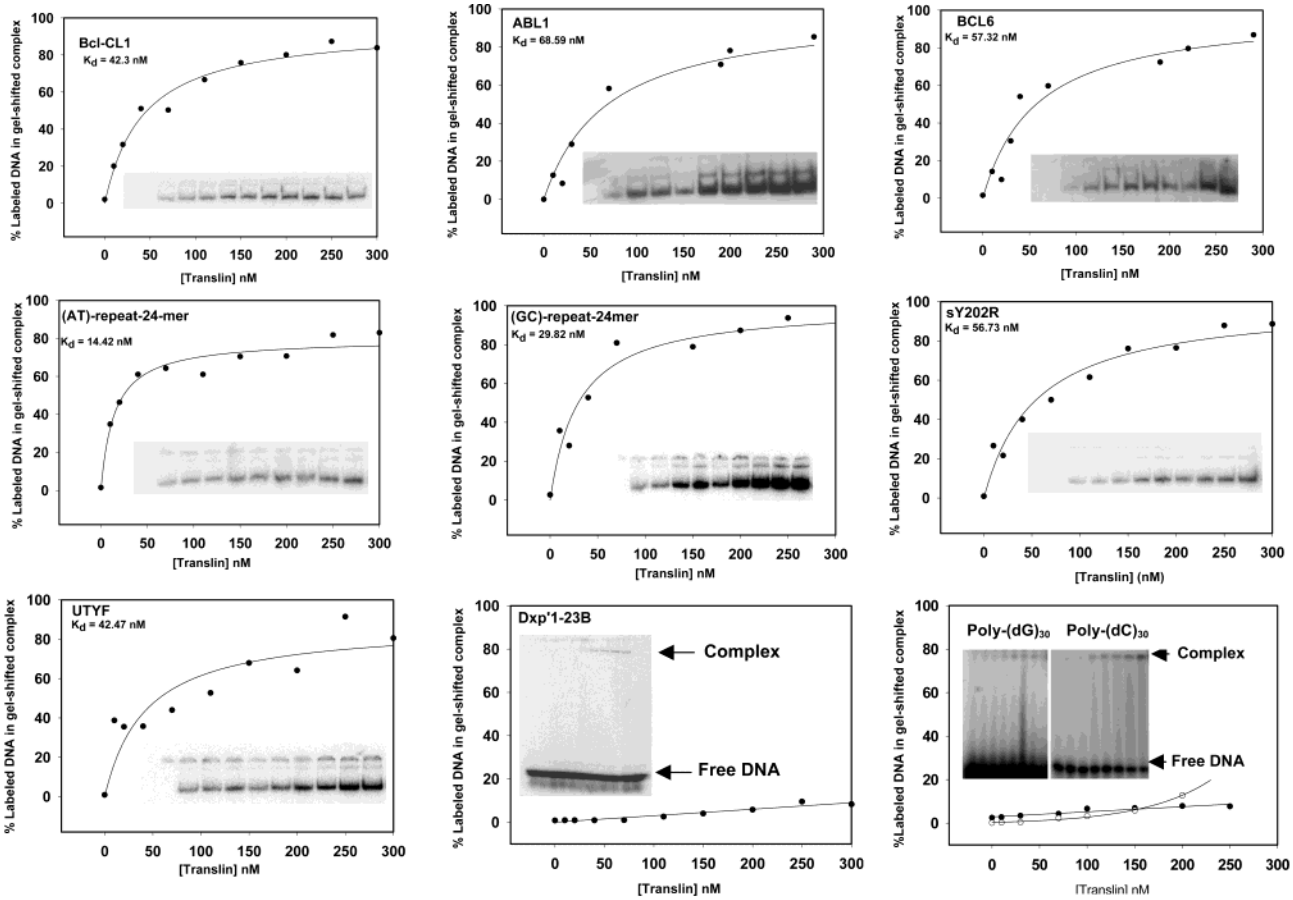

FIGURE 1: Electrophoretic mobility shift assays (EMSA) and quantitative analyses of the binding affinity of translin with breakpoint and nonbreakpoint sequences. The 5′-labeled oligonucleotide (80 nM, nucleotides) was incubated with increasing concentrations of translin for EMSA. The experimental conditions of binding assays and gel and quantitative analyses of the samples are as detailed under Materials and Methods. Each segment of EMSA analyses carries a gel autoradiogram [only gel-shifted complexes are shown as insets in panels belonging to Bcl-CL1, ABL1, BCL6, AT repeat, GC repeat, sY202R, and UTYF, whereas in panels belonging to Dxp′1-23B, poly(dG), and poly(dC) repeats, insets carry gel-shifted complexes as well as free DNA], binding isotherm, and the K_d value derived from the same. Symbols: (●) dG_{30}; (○) dC_{30}.

mM Tris-HCl (pH 7.5) (the buffer in which DNase I was dissolved) (minus DNase I control set) and incubated at room temperature for 2 min. The samples were subsequently quenched, denatured, and analyzed on a sequencing gel.

RESULTS

Short Consensus Motifs in Chromosome Breakpoint Junctions versus Translin Binding Affinity. The consensus sequences for chromosomal breakpoint junctions to which translin binds are not simple. Analyses suggest that the sequence variation in the breakpoint junctions is so large that the binding motifs in the targets are too short to be specific. In fact, it has been estimated that the short binding motifs of translin are expected to be present as widely in the genome as once in 57.1 bases (*2*). We conducted binding studies between translin and a set of bona fide breakpoint sequences (Bcl-CL1, ABL1, BCL6) as well as those that do not belong to any known bona fide breakpoint sequences. A variety of nonbreakpoint sequences were compared, comprising those that either had no known translin consensus breakpoint motifs, such as ATGCAG and GCCC(A/T)(G/C)(G/C)(A/T) (*1*, *2*) or those that had naturally occurring variants of the same. Simple repeat sequences (AT repeat, GC repeat) and a mixed sequence oligonucleotide (Dxp′1-23B) (used by others earlier for studying translin binding) (*1*) represented the former subgroup that had no consensus motif. In the second category with natural variants of the consensus motif, *s*equence *t*ag *s*ites from deletion-prone regions of human Y-chromosome were studied (sY202R and UTYF) (*20*, *21*). The sequence analyses revealed a motif, ACCCTACT, in sY202R that is related to translin binding consensus motif GCCC(A/T)(G/C)(G/C)(A/T) by two transition substitutions (at nucleotide positions 1 and 6). Similarly, UTYF has a motif, ATCTAG, that is related to consensus site ATGCAG by two transversions in the middle. All of these sequences whose binding affinity is being compared had a common fixed length (all 24mers) (Table 1). Binding was compared by performing gel shift analysis of a fixed concentration of 5′-γ-^{32}P-labeled oligonucleotide as a function of translin titration. Binding isotherms were generated by PhosphorImager quantification of gel-shifted complexes and the free DNA obtained at each protein concentration. The binding constants were retrieved from these isotherms using the Sigmaplot 5.0 program (Figure 1) (gel-shifted complexes are shown in all of the insets other than those of Dxp′1-23B and poly$(dG)_{30}$/poly$(dC)_{30}$, where free DNA also is shown). As expected and reported earlier for breakpoint sequences, the protein exhibited binding constants in the nanomolar range. The actual binding constants recovered were 42.3, 68.59, and 57.32 nM for Bcl-CL1, ABL1, and

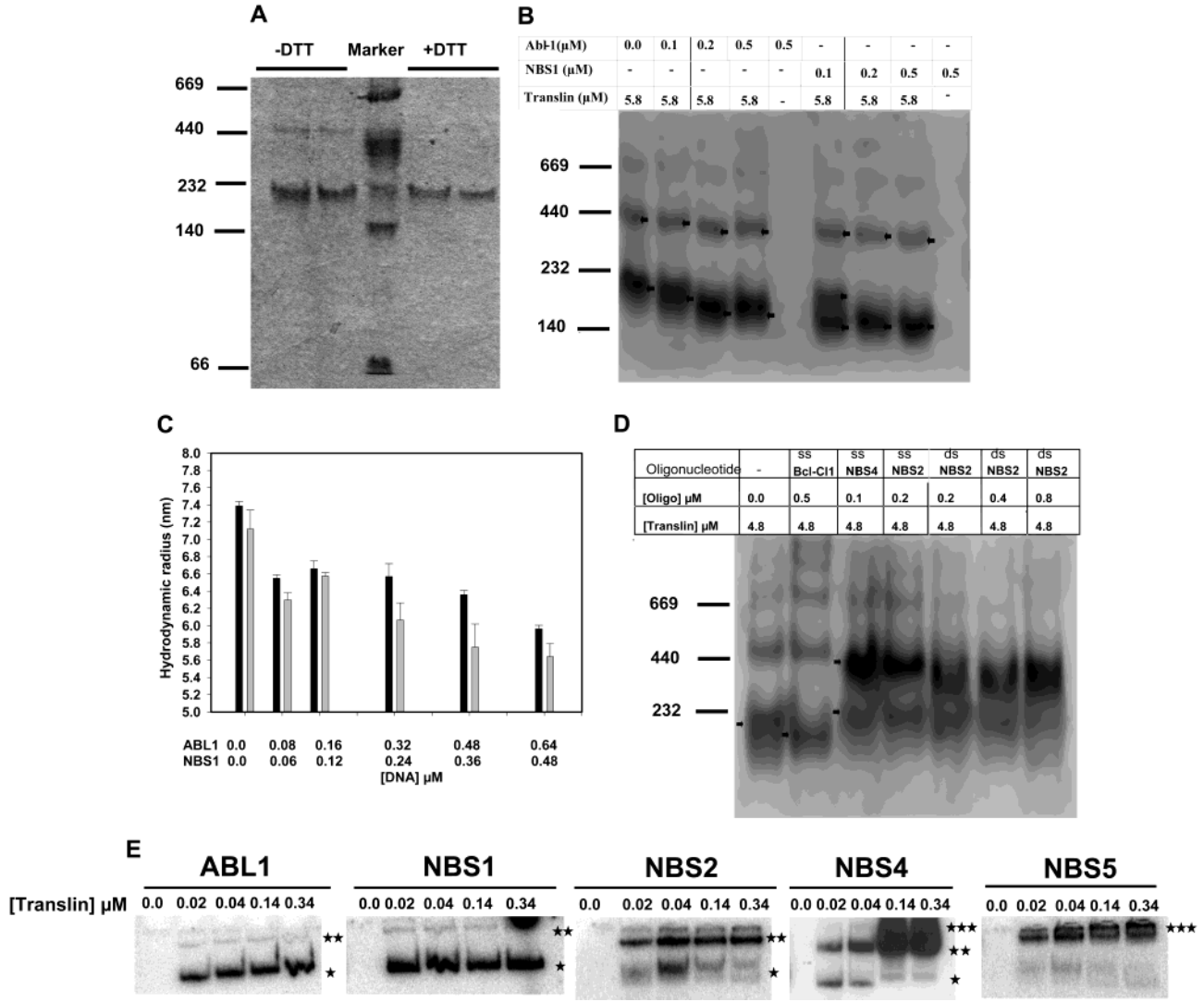

FIGURE 2: DNA-induced conformational changes in translin octamer states. (A) Native polyacrylamide gel analysis was performed in the absence of DNA to check the effect of DTT (1 mM) on the translin oligomeric state. Briefly, 100 μg of translin was loaded in each lane in the absence and presence of 1 mM DTT on a 5% native polyacrylamide gel and stained with Coomassie brilliant blue. The mobility positions of standard molecular weight markers are shown on the side. (B) The same analysis was repeated with 5.8 μM translin as a function of DNA titration (expressed as molecular concentration) (see Materials and Methods), followed by Ag staining to visualize the protein bands. Arrows indicate the mobility positions of translin double oligomer, oligomer, and conformationally altered oligomeric states. The mobility positions of standard molecular weight markers are shown on the side. (C) Evaluation of the hydrodynamic radius of the translin oligomer following DNA binding. Dynamic light scattering measurement (Materials and Methods) was carried out on translin (1.5 μM) that was incubated with various concentrations of either ABL-1 (gray bars) or NBS1 (black bars). DNA concentrations (expressed as molecular concentration) are shown below the respective bars. (D, E) Length effects of DNA targets on translin oligomeric states. (D) Translin (4.8 μM) was incubated with various oligonucleotide targets, followed by native polyacrylamide gel analysis and Ag staining to visualize the protein bands (see Materials and Methods) (molecular concentrations of strands are given) [single stranded (ss); double stranded (ds)]. Arrows indicate the mobility positions of the oligomer and double oligomer. (E) EMSA analyses of 5′-end-labeled ss-DNA targets of various lengths (Materials and Methods) (only gel-shifted complexes are shown). Single, double, and triple stars mark mobility positions of increasingly larger translin−DNA complexes.

BCL6, respectively (Figure 1). Surprisingly, the two repeat oligonucleotides (AT repeat and GC repeat) that had no homology with any known breakpoint sequences exhibited high binding affinity (14.42 and 29.82 nM, respectively), suggesting that DNA targets that apparently have no consensus, but confer a structural feature similar to that of consensus sequences, bind translin somewhat better than those of even bona fide consensus sites. On the contrary, Dxp′1-23B, which also had no known consensus motif, failed to elicit any appreciable binding. Even at high translin concentration, there was hardly any gel-shifted complex, which corroborated the binding behavior of this sequence reported earlier (*1*). The binding for this target in the concentration range of the protein tested was so low that no binding constant could be computed. Further, it is also pertinent to note that not all simple repeats are as good targets of translin binding as AT and GC repeats. This became clear when we observed that single-stranded oligonucleotides containing either A repeats, T repeats, G repeats, or C repeats showed hardly any binding to translin (data given only for C-30 and G-30, Figure 1) (note that this inset also contains free DNA along with that of shifted complexes). In the same conditions, the Y-chromosome oligonucleotides (sY202R and UTYF) exhibited binding affinity (56.73 and 42.47 nM, respectively) that was comparable to that of breakpoint sequences. The conclusion that small variations of consensus

can very well be tolerated during translin binding without any effect on binding affinity was further substantiated by other controls (data not given), where we studied sequences derived from M13 phage DNA that can be considered random with respect to that of a mammalian genome sequence (NBS1 and NBS4) (the former was part of the latter) (Table 1). Sequence search revealed that a single stretch of GACCTGCT (shown in bold, Table 1) found in both NBS1 and NBS4 was the best sequence match to the consensus motifs and was related to GCCC(A/T)(G/C)-(G/C)(A/T) by one transversion change at the second nucleotide. Gel shift analysis revealed that both of the oligonucleotides exhibited binding affinity (21.02 and 44.38 nM, respectively) similar to that of breakpoint sequences.

These binding comparisons with single-stranded DNA targets of the same size (24mer) suggest that translin binding is subject to complex effects that were not appreciated earlier where the binding affinity is not a simple and direct consequence of the consensus DNA motifs alone. Moreover, the binding studies, including that of longer targets such as NBS1 and NBS4, taken together, reiterate that a much larger variety of sequences than specified by bona fide breakpoints have the ability to attract translin at high affinity, thereby significantly enlarging the target base for translin binding in human genome (see Discussion).

Oligomeric State of Translin Vis-à-Vis DNA Binding. Electron microscopy and gel filtration chromatography as well as native PAGE analyses revealed an octamer state of human translin that was ss-DNA binding competent (*1*, *13*, *15*, *22*). On the other hand, glycerol gradient centrifugation experiment showed that TB-RBP, a close homologue of translin in mouse, binds DNA as a dimer (*14*). We wanted to evaluate this aspect by carefully analyzing the consequences of the translin oligomeric state following DNA binding. In our conditions also, as shown by others earlier, free translin in the denatured state migrated as a dimer when it was stabilized by disulfide linkage, which upon reduction by DTT was converted to a monomer (data not shown). However, in native conditions, the majority of the protein migrated as a species similar to that of the 232 kDa standard marker, suggesting an octameric state. In the same lane, trace amounts of the higher oligomeric state, comigrating with the 440 kDa marker, of translin (presumably, the double-octamer) were also found (Figure 2A). This was so whether the protein was reduced by DTT or not. To study the effect of DNA on the oligomeric state of the protein, we titrated a fixed amount of translin (5.8 μM monomer or $\sim$0.7 μM octamer) with increasing levels of a breakpoint (ABL1) or a nonbreakpoint sequence DNA (NBS1). This was followed by visualization of protein oligomers by silver staining in a native gel. At high enough concentrations of DNA that tend to saturate translin protein, the translin band (presumably corresponding to the octamer) was converted to a species that migrated faster than that of free protein (Figure 2B). Such a transition (indicated by arrows in the figure) was observed with both the breakpoint and the nonbreakpoint sequence DNA. In fact, at a subsaturating level of NBS1 (0.1 μM, expressed as molecular concentration), one could clearly observe the mixed population of translin consisting of the free octamer and the faster moving form of translin that is presumably DNA-bound. As the concentration of DNA increased further, even the residual free octamers got converted to the faster moving species, the migration of which was slower than that of the 140 kDa standard marker. Moreover, no additional, faster moving band of translin was observed in the lanes where DNA was added, presumably indicating that the translin oligomer (octamer) was not dissociated into two different suboligomers. In this experiment, the faster species represented either a conformational change induced in the original oligomeric state of the protein or its dissociation into similarly sized smaller particles (perhaps tetramers) or a combination of both effects, which cannot be distinguished in this technique, following DNA binding. To corroborate the DNA-induced effects observed in native gel migration, we analyzed the same in a more equilibrium assay by studying the hydrodynamic radii of translin as a function of DNA concentration using dynamic light scattering (DLS) in Dynapro LS. We studied DLS also at a micromolar concentration of translin similar to what we had used in native PAGE assays. At these conditions, DLS detected a predominant molecular species whose hydrodynamic radius (R_H) in various DLS runs fell within the range of 7.1−7.4 nm. Larger aggregates constituted only a very small percentage (<0.3%) of the total scatter, suggesting the paucity of such species in the sample. Although the hydrodynamic radius (R_H) measured for free protein is within the range of size estimates made by EM and previous DLS studies (*22*, *23*), it is not clear what the R_H value represents given the complex ellipsoid octameric ring shape translin exists in (*22*). Our main goal in using DLS was to measure the changes in R_H following the addition of DNA to translin. Translin protein was titrated with increasing concentrations of DNA (ABL1 or NBS1), followed by DLS measurement of R_H. Addition of either type of DNA (ABL1 or NBS1) led to a gradual fall in R_H (Figure 2C). Addition of DNA beyond $\sim$0.7 μM (molecular concentration) did not lead to any further drop in R_H (data not shown), suggesting that the average R_H recovered appears to have reached a plateau by about $\sim$0.5−0.6 μM DNA. In parallel, the total intensity of scattered light by the protein, which is proportional to $(R_H)^6$, also showed an appropriate level of decline as a function of DNA added (data not shown), corroborating that the size of the Raleigh scattering particle in the presence of DNA (translin−DNA complex) was less than that of free translin. Within the observed standard deviation in the measurements, the drop in R_H caused by ABL1 was marginally greater than that of NBS1. A drop in translin R_H following its saturation with DNA from about 7.1−7.4 nm to about 5.6−6.0 nm reflected a significant change in the original oligomeric state of translin, a situation that points to either a strong conformational change or the dissociation of translin oligomers. Thus DLS measurements are consistent with the mobility shift of translin oligomers observed in native gels following DNA binding. DNA-induced changes in translin were studied with other DNA targets as well. Translin mobility was analyzed in the presence of either NBS4 (83mer ss-DNA) or NBS2 (as 61mer ss-DNA or 61 bp duplex DNA). The observed effects on translin migration with these DNA substrates were markedly different from those observed with shorter ss-DNA fragments. Even at concentrations of DNA (0.1 μM molecule) that were subsaturating with respect to translin oligomers (4.8 μM monomers amounting to about 0.6 μM octamer), the majority of the translin oligomers were shifted toward slower electrophoretic migration (Figure 2D),

an effect contrary to what was observed in the previous experiment (Figure 2B). The retardation in the mobility of the translin oligomer ensued with all three longer DNA substrates tested (ss-DNA NBS4, ss-DNA NBS2, and ds-DNA NBS2) (Figure 2D). A 2-fold and 4-fold increase in NBS2 duplex concentration that approaches the stoichiometry of translin oligomers (octamers) only marginally enhanced this effect where almost the entire population of translin exhibited a slower electrophoretic migration (Figure 2D). A simple interpretation of slower migration of translin in this experiment is that translin oligomers may be aggregating on longer DNA substrates, presumably into double/triple octamers. We surmised that the octameric rings being loaded on longer DNA targets might be getting aggregated (stacked) into double/triple octamers, giving rise to slower electrophoretic migration. If this thinking is right, conversely, if we monitor translin binding by gel retardation assay using labeled DNA targets, aggregation of translin oligomers should result in supershifted complexes, the level of which should depend on the length of the target DNA strand. We tested this proposition by performing gel retardation assay under gel conditions where the translin−DNA complexes are resolved well. We did this experiment as a function of DNA strand length as well as translin concentration. Importantly, the length effect was analyzed on strands that shared the same common central core sequences, harboring a variant of consensus site GACCTGCT (described in Figure 1). In this set of oligonucleotides (NBS1, NBS2, NBS4, and NBS5; see Table 1), NBS1 is a part of NBS2, which in turn is part of NBS4, which forms the central casette of NBS5. Therefore, comparison of translin complexes on this set of DNA strands, which are mutually related to one another by sequence commonness, reduces the sequence context effects on translin binding. It is also relevant to point out here that earlier binding affinity measurement on NBS1 and NBS4 (described earlier in the text, 21.02 and 44.38 nM, respectively) strongly suggested that this set of strands provides a high affinity target site for translin to study the length effects on translin loading. Under the conditions of the assay, we detected three discrete gel-shifted complexes (only gel-shifted complexes are shown with stars, Figure 2E). When the target DNA used was small as in the case of NBS1 (or ABL1, used as a breakpoint control), the relative ratio of these three complexes hardly changed as a function of translin concentration. On the contrary, there was a gradual drop in the level of faster moving gel-shifted complexes (smaller complexes) with a concomitant increase in the slower ones (larger complexes), as the translin load increased on longer strands, an effect that is consistent with translin aggregation induced by the high concentration of protein on longer target strands. In fact, the length dependence of this effect was evident by the result that while the conversion of smaller complexes (single star) into the larger ones (double star) at intermediate concentration of translin (20 nM−140 nM) was only partial on NBS2, the same went not only to completion but also to much larger complexes (triple stars, Figure 2E) on NBS4 due to its longer length. In fact, the length effect was so pronounced on NBS5 that the complexes formed were of larger type (triple stars) even at the lowest concentration of translin (20 nM), perhaps reflecting an inherent cooperativity among translin oligomers while loading on long targets.

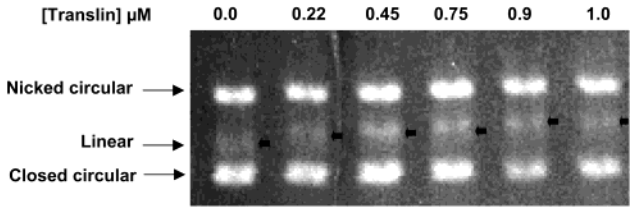

FIGURE 3: Translin is a duplex−DNA end binding protein: EMSA with plasmid DNA targets. Partially digested pGEM7Z (3.5 μg) was incubated with translin at the indicated concentrations, resolved on a 0.7% agarose gel, and stained with ethidium bromide (Materials and Methods). Arrows indicate the mobility of linear DNA as a function of translin concentration.

Translin Loads onto Linear Duplexes via the DNA Ends. One of the interesting models that can rationalize the strand length dependent effects of translin loading on DNA targets described in Figure 2E involves loading of translin oligomers through the free ends of DNA, a property that has been shown earlier by others by EM (*22*). To test this biochemically on a target duplex, we did the following binding assay using plasmid DNA, where it is possible to generate controls of the same target in circular forms. In a partial digest of a restriction enzyme, three different forms of plasmid duplexes, namely, supercoiled, nicked circular, and linear, were recovered. Such a mixture of plasmid forms was incubated with increasing amounts of translin, followed by agarose gel electrophoresis to detect the mobility shifts caused by translin binding. Interestingly, in each lane that contained all three forms of duplex plasmid, only the linear duplex exhibited gel retardation, the extent of which was highly dependent on the input concentration of translin. It is pertinent to mention here that the mobility retardation of the linear DNA band was continuous as a function of protein concentration (indicated by the arrows in Figure 3). This result suggested that translin oligomers were sequentially loaded through the free ends of DNA, an effect consistent of a ring-shaped protein oligomer. To get some insights on the structural state of the DNA double helix that is encased within translin rings, we designed an assay that measures the level of DNA end-breathing and assessed the same in DNA ends trapped with translin rings.

Translin Oligomers "Clamp" the Duplex Ends against the Effects of End Fraying. The fraying open or breathing of DNA ends is an important, but hitherto not well appreciated, physical property of a linear duplex that DNA end binders might modulate. We wanted to assess this parameter using a classical DNA branch migration assay. The basic premise of the assay rests on the fact that the nascent single strandedness that is generated in a duplex DNA due to breathing of ends can be captured by pairing induced by the large molar excess of complementary strands. Such a pairing event between duplex DNA and one of its complementary strands initiates the formation of a three-stranded branch that can freely migrate isoenergetically across the region of sequence homology. When a large molar excess of the unlabeled strand is added to the duplex DNA that contains the same as the labeled strand, branch migration is initiated, leading eventually to the displacement of the labeled strand from the duplex, the steady-state level of which can be monitored on a native gel. We assayed this effect on two different substrates: one that is a fully blunt-ended duplex (NBS2) and the other a tailed duplex where the same 61mer

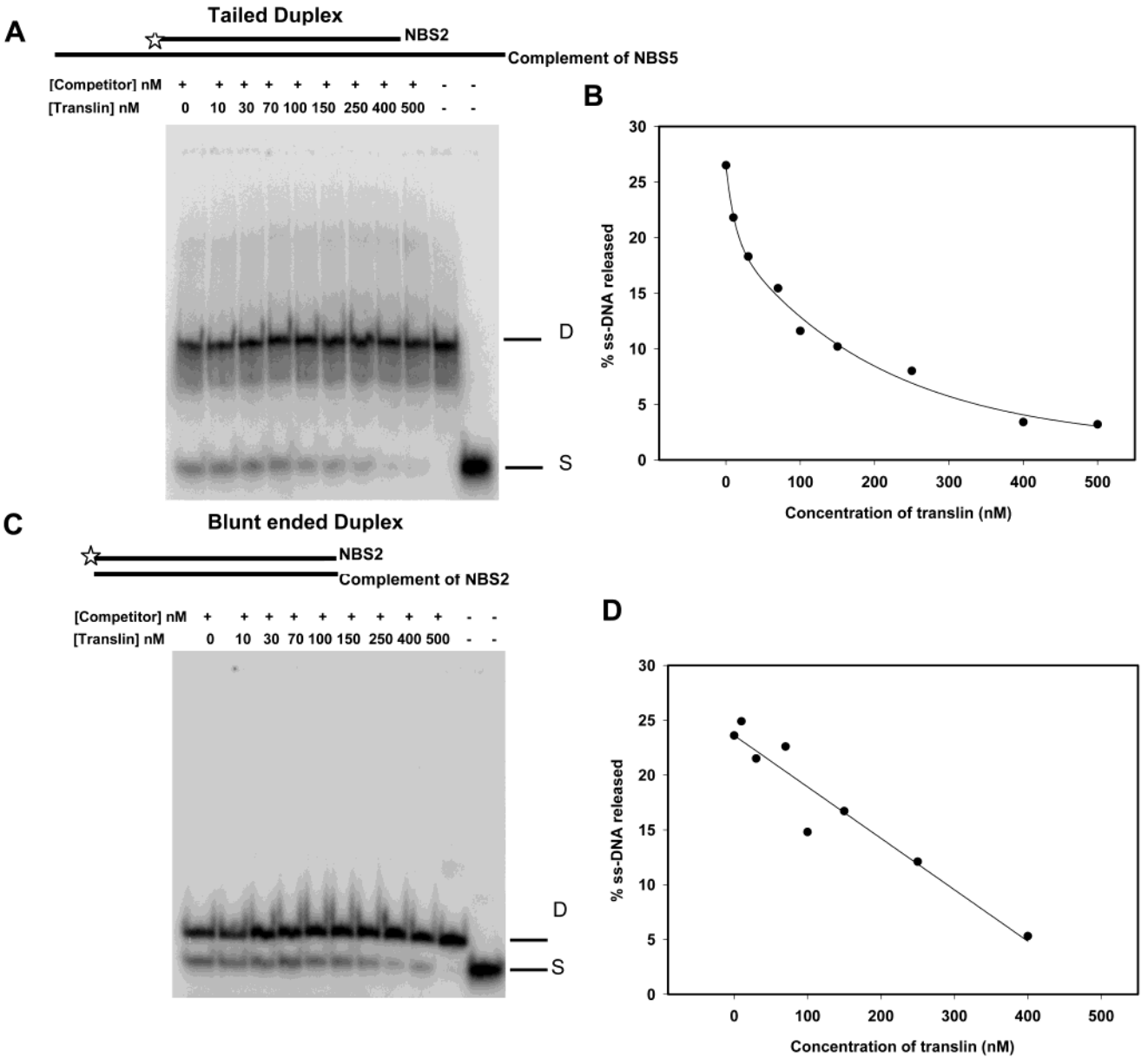

FIGURE 4: DNA duplex ends are clamped by translin binding: end-clamping assay. Duplex DNA substrate containing annealed labeled NBS2 was incubated with translin at the indicated concentrations and further challenged with a 6-fold molar excess of unlabeled NBS2, followed by native polyacrylamide gel analysis of naked DNA products (see Materials and Methods). (A, B) Tailed duplex substrate between labeled NBS2 and the complement of NBS5. (C, D) Blunt-ended duplex substrate between labeled NBS2 and its own complement. D and S on the side indicate the positions of the duplex and ss-DNA, respectively. Graphs in (B) and (D) are derived from the PhosphorImager quantitation of radioactive bands in (A) and (C), respectively.

strand was annealed to the complement of NBS5 (121mer), thus generating 30mer long tails on either side of an internal 61 bp duplex. In both substrates, the same 61mer was labeled at the 5′ end. Both duplexes were completely free of any contaminating unannealed labeled 61mer single strands (see the second lanes from the right in Figure 4A,C). As expected from the effects of branch migration described above, when a 6-fold molar excess of the unlabeled competitor 61mer single strand was incubated with either labeled duplexes, about 25% of the annealed labeled strands in the duplexes were branch migrated off, as observed by the release of the same (see lanes with no translin, Figure 4A,C). This was the steady-state level of branch migration observed under the conditions of the assay, as no labeled single strands were released if the duplexes were challenged with an equivalent molar excess of nonhomologous competitive 61mer strands (second lanes from the right in Figure 4A,C). So the method was scoring the fraying ends of the DNA as a branch migration assay. We repeated the same assay after loading the translin on the duplex, followed by the addition of a molar excess of unlabeled competitor 61mer single strands. The experiment was done as a function of protein concentration to assess the translin dose−response pattern, if any. In both experiments, addition of translin led to inhibition of strand displacement, which was translin concentration dependent (Figure 4). At the highest concentration of translin, the level of strand displacement measured was similar to that of the background level of radioactivity observed in the gel, indicating that branch migration was inhibited almost completely. Interestingly, the translin concentration dependence of the inhibition of branch migration was measurably different for the tailed duplex versus the blunt-ended duplex,

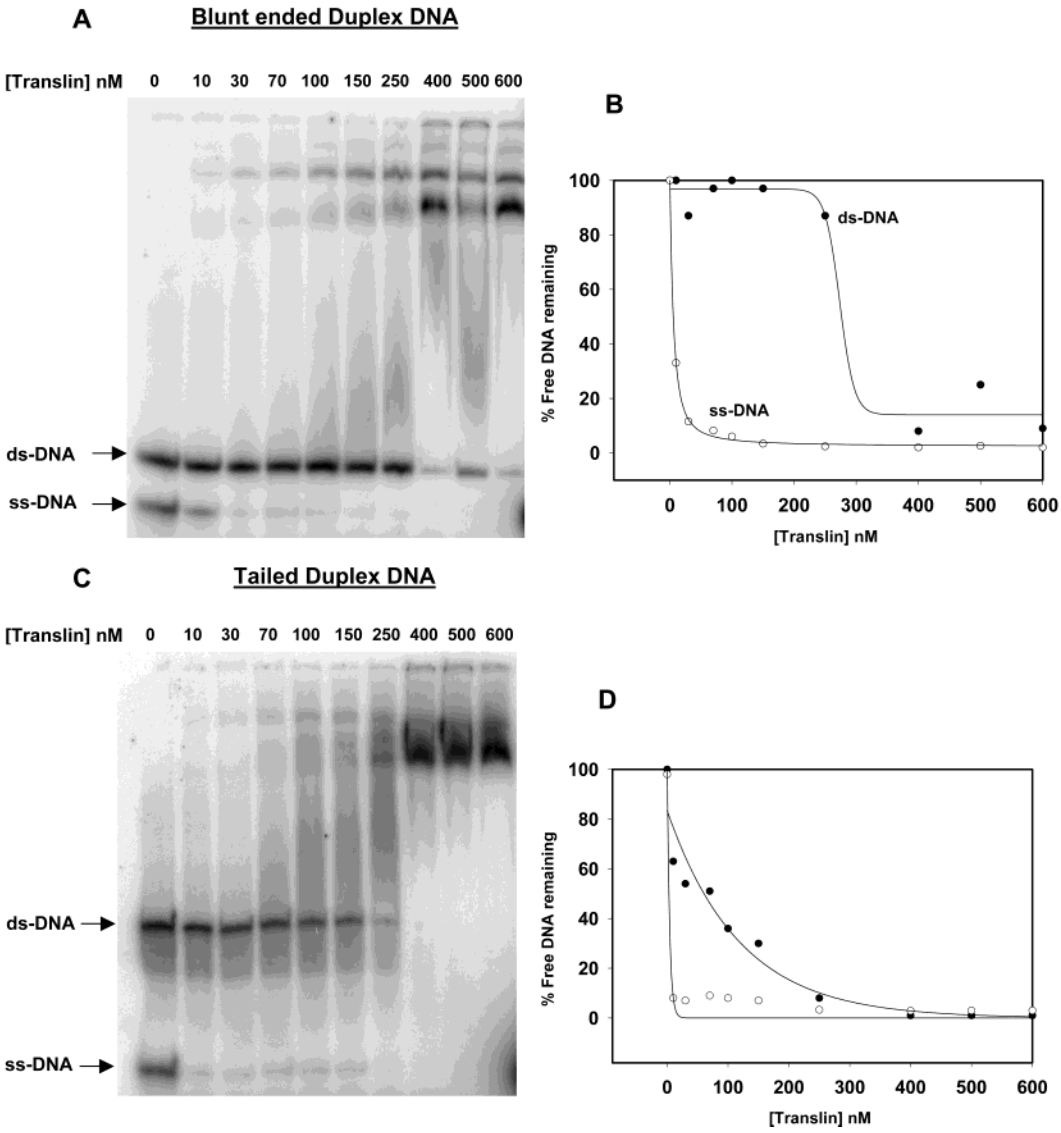

FIGURE 5: Translin binding to the single strand, tailed duplex, and blunt-ended duplex. As in Figure 4, tailed duplex and the blunt-ended duplex substrates were formed by annealing labeled NBS2 with the complement of NBS5 and NBS2, respectively (see Materials and Methods). A mixture of such a duplex DNA (blunt ended or tailed) (1.3 nM molecules) and labeled NBS2 (0.87 nM molecule) was incubated with translin at the indicated concentrations, followed by native polyacrylamide gel analysis for gel shift analyses (see Materials and Methods). ds-DNA and ss-DNA on the side indicate the positions of duplex and ss-DNA, respectively. Graphs in (B) and (D) are derived from the PhosphorImager quantitation of radioactive bands of ss-DNA and ds-DNA in (A) and (C), respectively. Radioactivity associated with these bands in translin lanes is expressed with respect to that in the first lane (containing no translin), which is considered as 100%. These values are plotted as the percentage of free DNA remaining against the translin concentration. Closed and open circles represent ds-DNA and ss-DNA, respectively.

even though both shared the same duplex sequence. At a low concentration of translin, the abrogation of branch migration was more marked with tailed duplex DNA than that with the blunt-ended duplex, suggesting that the single strands in the tailed duplexes conferred a higher affinity site for translin loading. At high enough concentration of translin, both duplexes showed a similar level of inhibition in branch migration. This experiment suggests that loading of translin oligomers on the duplex ends generate a "clamping effect" on duplex ends that manifests as a reduction in branch migration levels. We discuss further the implications of such a result in relation to translin function.

Translin Binding Affinity to Single Strand versus Blunt-Ended/Tailed Duplex. In the preceding experiment, there was an indication that the binding effect on a duplex end manifests at a much lower concentration of translin when it is part of a tailed duplex than when it is a blunt-ended duplex. To assess whether it is a direct consequence of difference in the binding affinity, we carried out binding analyses of the same using gel shift analyses. The substrates used were the same as in the previous experiment, where the labeled NBS2 strand was annealed to its complement to generate either a blunt-ended or a tailed duplex (see cartoon, Figure 4). In this experiment, we premixed either duplexes with labeled NBS2 single strands prior to translin binding, so as to provide an internal single strand control for comparison in the gel shift analyses. Thus, in these two different mixtures, about 40% of the label was contributed by NBS2 single strands and the remaining 60% by either blunt-ended duplex or tailed duplex substrate (see first lanes in Figure 5A,C). Gel shift analyses were performed as a function of translin titration. Since gel-shifted complexes are contributed by either substrates, to assess the translin binding to DNA substrates separately in a given sample mixture, we quantified the

relative loss of labeled substrates as a function of translin binding. Since, in a given set, all lanes were loaded with binding mixtures that carried the same amount of labeled substrates, we measured the labeled substrates that remained free following translin binding and expressed the same as a percentage of starting substrate where no translin was added. By this method, in the same set, we could assess the relative binding affinity of the single strand as well as the same in the duplex form simultaneously. As expected of a single strand in this category, NBS2 exhibited a high binding affinity where, by the addition of 70−100 nM translin, most of the labeled strand was converted into complexes, showing no free leftover strands in the gel, revealing a high-affinity binding constant of translin (nanomolar range) with NBS2 (Figure 5). This was so in either binding experiment (Figure 5B,C), proving that NBS2 served as a good internal control. Interestingly, however, in the same analyses, duplex substrates behaved markedly different: while most of the tailed duplexes were shifted by about ∼250 nM translin, that of blunt-ended duplexes required about ∼400 nM translin. In addition, a significant level of binding to tail duplexes ensued at a much lower concentration (∼70−150 nM) of translin than that observed with blunt-ended duplexes where gel shift ensued only at a much higher concentration (∼200−300 nM) of translin. These results, taken together, strongly suggest that a target of the DNA strand is much better recognized by translin when it is presented as a single strand, as compared to the same either as the blunt-ended or as the tailed duplex. Moreover, among the two types of duplexes, translin binding is significantly better with a tailed duplex as compared to that of blunt-ended duplex, a result that can elegantly rationalize the contrasting dose-dependent effects of translin in promoting the "clamping" of the same duplex ends when it is part of blunt-ended or tailed duplex substrates (Figure 4).

Single Strands Covered by Translin Are Rendered Hypersensitive to DNase I. What is the conformational status of the single-stranded DNA that is captured by translin oligomers? To get an insight on the same, we probed the 5′-end-labeled NBS4 strand covered by translin with DNase I, a nonspecific endonuclease. Under the conditions of limited digestion, DNase I introduces nicks all along the strand endonucleolytically, during which many proteins that tightly wrap the DNA backbone exhibit classical protection against nicking, referred to as "DNase I footprints". We titrated NBS4 with increasing concentrations of translin protein, followed by limited DNase I digestion. Interestingly, the experiment revealed that the strand was rendered hypersensitive to DNase I as a function of translin concentration (Figure 6). The digestion level was marginally higher at a low concentration of protein, the extent of which was markedly elevated when the concentration of translin was high enough to saturate all single-stranded DNA molecules. As an important control, we repeated the same experiment without DNase I to check whether the effect of digestion was a simple effect of translin preparation itself. In this control, the labeled strand remained intact at all translin concentrations tested where no detectable strand nicks were observed even at the highest protein concentration (Figure 6). We observed a similar hypersensitivity to DNase I following translin coverage when the same strand was in the duplex state as well (data not shown). These results revealed that DNase I

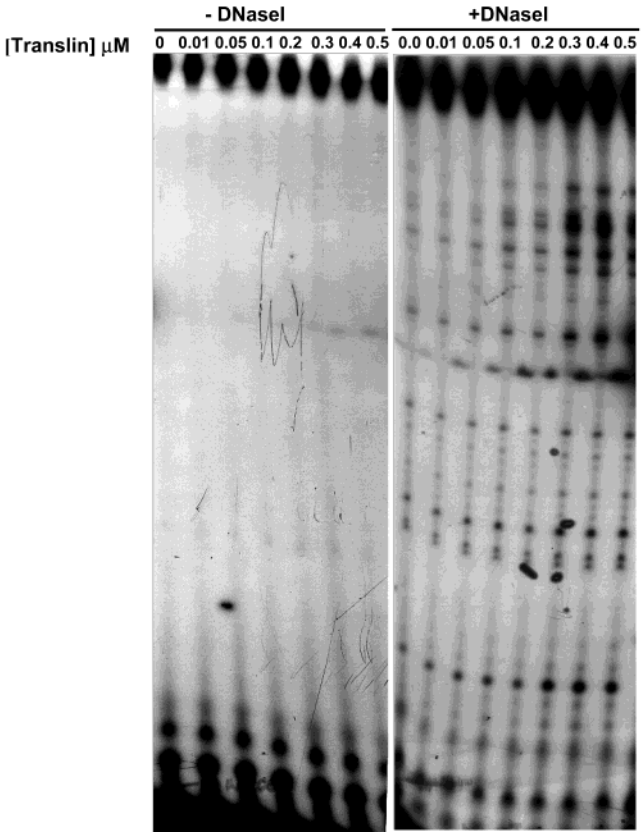

FIGURE 6: Translin binding renders the ss-DNA target hypersensitive to DNase I action. The 5′-end-labeled NBS4 (0.5 μM nucleotide) was coated with increasing levels of translin, followed by DNase I probing and analyses of the products on a sequencing gel (see Materials and Methods).

hypersensitivity exhibited by the DNA strand encased in translin rings is genuinely due to its significantly altered state of conformation vis-à-vis the same when it is naked, an effect that is potentially very relevant in the biology of translin.

DISCUSSION

Human translin was initially isolated as a protein that binds to translocation breakpoint sequences in hematopoietic malignancies (*1*). However, the molecular mechanism that can describe the precise role of translin in chromosomal translocations is completely unclear. This is also because the details of molecular events starting from the initiation and processing of DSB's to the generation of new chromosomal joints during any translocation event are very rudimentary. The complexity of the process at the DNA level is compounded further following recent revelations that chromosome translocations are generally not simple end-to-end joining events but also involve gain or loss of sequences (*24*).

We first addressed the issue of the specificity of translin binding to known breakpoint sequences. This issue, which appeared simple, turns out to be more complex for the following reasons. Sequence variation in the known cases of breakpoint junctions is so large that the consensus motifs in the targets get too short to be specific. In fact, it has been estimated that the short consensus motifs of translin are expected to be as widely prevalent in the genome as once in 57.1 bases (*2*). Translin protein seems well evolved not only

to bind to such short consensus motifs but also to recognize the sequence variants of the same equally well (Figure 1). Intriguingly, the protein seems to bind certain simple sequence repeats (AT repeat and GC repeat) with a higher affinity than consensus sites themselves (Figure 1). Moreover, the protein also seems to modulate its affinity to the same sites depending upon whether they are part of a blunt-ended or tailed duplex (Figure 5). These properties of translin seem to suggest that it has evolved to bind very efficiently a large repertoire of short stretches of single-stranded DNA that might stochastically emerge during breakage events anywhere in the genome.

Regardless of the nature of translocation, i.e., reciprocal or nonreciprocal, the underlying process at some point must involve either DNA double strand breaks (DSB) or two nearby single strand breaks. The cells are endowed with two robust machineries in the form of nonhomologous end joining (NHEJ) and homologous recombination (HR) pathways to maintain chromosomal stability against the constant barrage of spontaneous DNA double strand breaks (*25*). Expectedly, cells deficient in component(s) in the NHEJ pathway exhibit a large number of translocations that resemble the classic translocations found in Burkitt's lymphomas and mouse plasmacytomas (*26*). A crucial question then asked is what cellular apparatus generates translocations in the compromised cases of NHEJ? This is a question whose answer might also provide insights as to what new molecular events might have "tricked" the NHEJ pathway into giving rise to chromosomal translocations in a wild-type setting, off and on. Are translin and trax proteins, which do not belong to either NHEJ or HR pathways, such new candidates that most likely somehow "trick" NHEJ into a misrepair function, thereby generating the chromosomal translocation? This notion is consistent with the recent proposal that the NHEJ pathway that is so important for cell survival may itself be tricked into generating potentially fatal translocations (*25*). The results obtained in the current study, though entirely in vitro, have some suggestions in that direction with respect to the role of translin, which are summarized below.

Translin, which has been demonstrated by others and reiterated in the current study to exist as a stable octamer, is subject to interesting conformational changes following its interaction with DNA targets. The translin octamer seems to compact itself upon binding to short single strands (Figure 2B,C), where it perhaps complexes in 1:1 stoichiometry (*27*), a result perfectly consistent with image reconstruction data reported earlier (*22*). However, when the target DNA is increased, more octamers (double, triple, etc., Figure 2E) seem to align onto the same strand, giving rise to a DNA conformation that is now rendered hypersensitive to a nuclease (Figure 6). A comparable situation arises where translin octamers that recruit themselves on double-stranded DNA target sequentially via the free ends (Figure 3) and transform the double helical DNA into a configuration where the strands are more tightly clamped at the ends (Figure 4).

Translin under constitutive conditions is cytoplasmic in its localization due to its nuclear export signal (*1*, *6*). During the stages of either natural genome rearrangements (such as that of immunoglobulin and T cell receptor genes in cells of hematopoietic origin) or accidental chromosomal translocations (*1*) and damage-induced DNA repair settings (*13*), translin is nuclearly recruited by the help of the trax protein (*6*, *28*). Trax seems to be its physiological regulator that lowers translin affinity toward RNA targets and concomitantly elevates translin affinity toward DNA targets (*6*). In this model, it is conceivable that the DNA strands thread into the rings of the translin octamer, while the trax presumably complexes on the outside surface of translin. The recent crystal structure of TB-RBP, a mouse orthologue of translin, clearly reveals that DNA binding sites reside in the inside surface of the octameric structure (*29*). It is in this setting that interesting molecular matchmaking roles of trax might kick in, where it succeeds in matchmaking DNA-dependent protein kinase to translin via its mediator C1D (*30*), which is a known interactor as well as activator of DNA-dependent protein kinase (*31*) in a manner that obviates the requirement of Ku protein. We propose here that entry of DNA-dependent protein kinase into a translin pathway at chromosomal ends is thus feasible that now imbalances the classical NHEJ pathway leading to aberrant repair in the form of translocations. We believe that this model, although very preliminary at this stage, facilitates interesting testable propositions that will provide more precise molecular functions for translin and trax in chromosome translocation events.

ACKNOWLEDGMENT

We thank Dr. M. Kasai, Department of Immunology, National Institute of Health, Tokyo, Japan, for kindly providing the overexpression clone of human translin, Prof. G. Krishnamoorthy, Department of Chemical Sciences, TIFR, for help in DLS experiments, and Amita Joshi and Sunita Ramanathan for critical input.

REFERENCES

1. Aoki, K., Suzuki, K., Sugano, T., Tasaka, T., Nakahara, K., Kuge, O., Omori, A., and Kasai, M. (1995) *Nat. Genet. 10*, 167−174.
2. Hosaka. T., Kanoe, H., Nakayama, T., Murakami, H., Yamamoto, H., Nakamata, T., Tsuboyama, T., Oka, M., Kasai, M., Sasaki, M. S., Nakamura, T., and Toguchida, J. (2000) *Oncogene 19*, 5821−5825.
3. Wu, X. Q., Gu, W., Meng, X., and Hecht, N. B. (1997) *Proc. Natl. Acad. Sci. U.S.A. 94*, 5640−5645.
4. Wu, X. Q., Lefrancois, S., Morales, C. R., and Hecht, N. B. (1999) *Biochemistry 38*, 11261−11270.
5. Hasegawa, T., and Isobe, K. (1999) *Biochim. Biophys. Acta 5*, 161−168.
6. Chennathukuzhi, V. M., Kurihara, Y., Bray, J. D., and Hecht, N. B. (2001) *J. Biol. Chem. 276*, 13256−13263.
7. Chennathukuzhi, V. M., Kurihara, Y., Bray, J. D., Yang, J., and Hecht, N. B. (2001) *Nucleic Acids Res. 29*, 4433−4440.
8. Haber, J. E. (2000) *Curr. Opin. Cell Biol. 12*, 286−292.
9. Jeggo, P. A. (1998) *Radiat. Res. 150*, S80−S91.
10. Jeffs, A. R., Benjes, S. M., Smith, T. L., Sowerby, S. J., and Morris, C. M. (1998) *Hum. Mol. Genet. 5*, 767−776.
11. Atlas, M., Head, D., Behm, F., Schmidt, E., Zeleznik-Le, N. H., Roe, B. A., Burian, D., and Domer, P. H. (1998) *Leukemia 12*, 1895−1902.
12. Chalk, J. G., Barr, F. G., and Mitchell, C. D. (1997) *Oncogene 15*, 1199−1205.
13. Kasai, M., Matsuzaki, T., Katayanagi, K., Omori, A., Maziarz, R. T., Strominger, J. L., Aoki, K., and Suzuki, K. (1997) *J. Biol. Chem. 272*, 11402−11407.
14. Wu, X. Q., Xu, L., and Hecht, N. B. (1998) *Nucleic Acids Res. 26*, 1675−1680.
15. Aoki, K., Suzuki, K., Ishida, R., and Kasai, M. (1999) *FEBS Lett. 443*, 363−366.
16. Karthikeyan, G., Wagle, M. W., and Rao, B. J. (1998) *FEBS Lett. 425*, 45−51.

17. Sambrook, J., Fritsch, E. F., and Maniatis, T. (1989) *Molecular Cloning: A Laboratory Manual*, p 11.39, Cold Spring Harbor Laboratory Press, Plainview, NY.
18. Joshi, A., and Rao, B. J. (2002) *Biochemistry 41*, 3654−3666.
19. Kamp, C., Hirschmann, P., Voss, H., Huellen, K., and Vogt, P. H. (2000) *Hum. Mol. Genet. 9*, 2563−2572.
20. Tilford, C. A., Kuroda-Kawaguchi, T., Skaletsky, H., Rozen, S., Brown, L. G., Rosenberg, M., McPherson, J. D., Wylie, K., Sekhon, M., Kucaba, T. A., Waterston, R. H., and Page, D. C. (2001) *Nature 409*, 943−945.
21. Blanco, P., Shlumukova, M., Sargent, C. A., Jobling, M. A., Affara, N., and Hurles, M. E. (2000) *J. Med. Genet. 37*, 752−758.
22. VanLoock, M. S., Yu, X., Kasai, M., and Egelman, E. H. (2001) *J. Struct. Biol. 135*, 58−66.
23. Pascal, J. M., Chennathukuzhi, V. M., Hecht, N. B., and Robertus, J. D. (2001) *Acta Crystallogr., Sect. D: Biol. Crystallogr. 57*, 1692−1694.
24. Kanoe, H., Nakamata, T., Hosaka, T., Murakami, H., Yamamoto, H., Nakashima, Y., Nakayama, T., Tsuboyama, T., Nakamura, T., Ron, D., Sasaki, M. S., and Toguchida, J. (2000) *Oncogene 19*, 5821−5825
25. Ferguson, D. O., and Alt, F. W. (2001) *Oncogene 20*, 5572−5579.
26. Korsmeyer, S. J. (1992) *Annu. Rev. Immunol. 10*, 785−807.
27. Lee, S. P., Fuior, E., Lewis, M. S., and Han, M. K. (2001) *Biochemistry 40*, 14081−14088.
28. Aoki, K., Ishida, R., and Kasai, M. (1997) *FEBS Lett. 401*, 109−112.
29. Pascal, J. M., Hart, J. P., Hecht, N. B., and Robertus, J. D. (2002) *J. Mol. Biol. 319*, 1049−1057.
30. Erdemir, T., Bilican, B., Oncel, D., Goding, C. R., and Yavuzer, U. (2002) *J. Cell Sci. 115*, 207−216.
31. Yavuzer, U., Smith, G. C. M., Bliss, T., Werner, D., and Jackson, S. P. (1998) *Genes Dev. 12*, 2188−2199.

BI026378M